Ferroxime(II)-catalysed oxidation of 3,5-di-*tert*-butylcatechol by O₂. Kinetics and mechanism†

Tatiana L. Simándi and László I. Simándi *

Chemical Research Center, Institute of Chemistry, Hungarian Academy of Sciences, H-1525 Budapest, PO Box 17, Hungary. E-mail: simandi@cric.chemres.hu

The complex [Fe(Hdmg)₂(MeIm)₂] **1**, referred to as ferroxime(II), was found to be the precursor of a selective catalyst for the oxidative dehydrogenation of 3,5-di-*tert*-butylcatechol (H₂dbcat) to the corresponding 1,2-benzoquinone (dtbq) at room temperature and atmospheric dioxygen pressure. The observed kinetic behaviour in MeOH is consistent with solvolysis of one MeIm ligand and binding of dioxygen to the five-co-ordinate intermediate to form a superoxo complex. The latter abstracts an H atom from H₂dbcat *via* a hydrogen-bonded ternary active intermediate, affording the semiquinone anion radical dbsq˙⁻ and [Fe^{III}(Hdmg)₂(MeIm)(O₂H)]. Utilising an electron and a proton from H₂dbcat, the latter undergoes heterolytic cleavage to yield a ferryl species, which rapidly oxidises a second H₂dbcat. Complexation of dbsq˙⁻ with [Fe^{II}(Hdmg)₂(MeIm)] affords a strongly coloured paramagnetic species [Fe^{II}(Hdmg)₂(MeIm)(dbsq˙⁻)], which persists throughout the catalytic reaction, acting as buffer for dbsq˙⁻. The proposed mechanism involves steps similar to those of the known cytochrome P450 cycle, with H₂dbcat acting as both ancillary electron source and substrate.

Introduction

There is continuing interest in modelling heme type iron complexes capable of dioxygen activation and catalytic oxidation.[1] A wide variety of iron porphyrin derivatives has been synthesized and tested for oxidation activity. They were expected to mimic the oxygenase activity of cytochrome P-450 and its selectivity in oxygen atom transfer reactions like epoxidation, and alkane and arene hydroxylation. Many of these expectations were fulfilled but oxidative decomposition of the porphyrin ring remained a drawback of these catalyst systems, although it was significantly suppressed in halogenated second and third generation porphyrin catalysts.[2,3]

The nature and modelling of active oxidising species in non-heme iron proteins prompted studies on the reduction of oxo-bridged diiron species derived from difluoro(dimethyl-glyoximato)borate[4,5] and on the autoxidation of bis(dimethyl-glyoximato)bis(imidazole)iron(II).[6]

In a search for square planar iron(II) complexes with 4N donor equatorial ligands, expected to mimic the porphyrin moiety, we have investigated the catalytic properties of bis(dimethylglyoximato)bis(*N*-methylimidazole)iron(II), [Fe(Hdmg)₂(MeIm)₂] **1**, for brevity also referred to as ferroxime(II) in this work. The starting point for this research was our earlier work on oxidations catalysed by cobaloxime(II) complexes.[7] We have found that [Fe(Hdmg)₂(MeIm)₂] activates dioxygen in MeOH solution at room temperature and catalyses the oxidative dehydrogenation of 3,5-di-*tert*-butylcatechol to the corresponding 1,2-benzoquinone (dtbq). We now report a detailed kinetic study of this reaction and interpret the observed kinetic behaviour in terms of a suitable reaction mechanism.

Experimental

The complex [Fe(Hdmg)₂(MeIm)₂] was synthesized by the procedure reported.[8] 3,5-Di-*tert*-butylcatechol (H₂dbcat) was an Aldrich product.

The catalytic reaction was carried out in methanol solution. Its progress was followed by HPLC, gas volumetry and UV-VIS spectrophotometry.

Rates of dioxygen uptake were measured in a constant pressure gas-volumetric apparatus described earlier.[7] The reaction was started by dropping the solid ferroxime(II) catalyst precursor into a vigorously stirred, thermally equilibrated methanol solution of H₂dbcat from a sample holder manipulated from the outside. The rate of O₂ absorption was independent of the stirring rate, excluding eventual diffusion control effects. The oxidation was also followed by recording the time evolutions of UV-VIS spectra on Hewlett-Packard 8452A and 8453 diode array spectrophotometers. The IR spectra were recorded in KBr pellets on a Specord 75 spectrometer, ESR spectra on a JES-FE-3X spectrometer.

HPLC Analyses were performed on a Waters 991 system with a Diode Array Detector (silica column, Spherisorb 5µ, eluent methanol–water 80:20, elution rate 1.0 cm³ min⁻¹). Detection of dtbq at 280 nm (R_t = 6.8 min), H₂dbcat at 280 nm (R_t = 8.4 min). Calibration with 4 or 5 samples of different masses was reproducible within about 1%. Samples withdrawn from the reacting mixture for HPLC analysis were quenched by 11-fold dilution with MeOH before injection.

Results and discussion

Stoichiometry and intermediates

Behaviour under N₂. According to parallel gas-volumetric and HPLC measurements, the stoichiometry of oxidation corresponds to eqn. (1). The mass balance required by it is

$$\text{H}_2\text{dbcat} + 0.5\text{O}_2 \longrightarrow \text{dtbq} + \text{H}_2\text{O} \qquad (1)$$
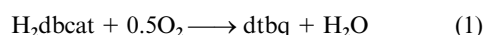
fulfilled within ±2%. No other oxidation products can be detected by HPLC or TLC.

Upon dissolution of [Fe(Hdmg)₂(MeIm)₂] **1** in methanol under N₂, the original pink colour rapidly changes to yellow. The successive spectra in Fig. 1(a) reveal that the characteristic

† *Supplementary data available*: rate data plotted in Fig. 4. For direct electronic access see http://www.rsc.org/suppdata/dt/1999/4529/, otherwise available from BLDSC (No. SUP 57680, 2 pp.) or the RSC Library. See Instructions for Authors, 1999, Issue 1 (http://www.rsc.org/dalton).

Table 1 First-order rate constant for the dissociation of MeIm from [Fe(Hdmg)$_2$(MeIm)$_2$] **1** in MeOH at 25 °C

Atmosphere	λ/nm	$10^2\,k$/s^{-1}
N$_2$	530	1.3 ± 0.05
	420	1.2 ± 0.05
	530	0.62 ± 0.03[a]
O$_2$	530	1.5 ± 0.05
	420	1.4 ± 0.04
[b]	360	0.014 ± 0.0006
[b]	530	0.011 ± 0.0004

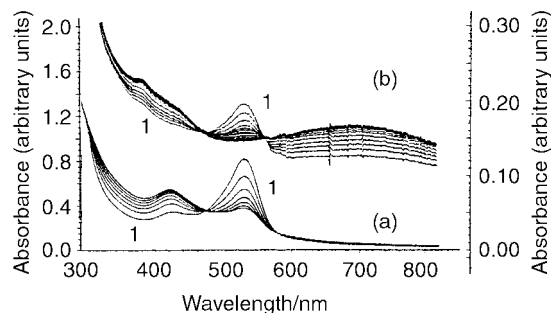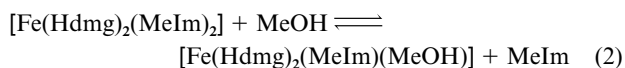[a] Dissociation in toluene, ref. 9. [b] Solvent: 10% MeIm in MeOH.

Fig. 1 Time evolution of UV-VIS spectra (15 s intervals) in MeOH at 25 °C ($l = 1$ mm). (a) Left-hand ordinate, under N$_2$, [Fe(Hdmg)$_2$(MeIm)$_2$]$_0$ = 2.29×10^{-3} mol dm^{-3}: (b) Right-hand ordinate, under air, [Fe(Hdmg)$_2$(MeIm)$_2$]$_0$ = 0.456×10^{-3}, [H$_2$dbcat]$_0$ = 19.25×10^{-3}, [O$_2$] = 2.27×10^{-4} mol dm^{-3}.

band of complex **1** at 530 nm[9] gradually disappears, while the 420 nm band increases due to the loss of co-ordinated MeIm by solvolysis according to eqn. (2). The three isosbestic points (at 290, 470 and 580 nm) indicate a single reaction and the bands at 530 and 420 nm can be assigned to **1** and **2**, respectively. First-order kinetics is observed at both wavelengths, yielding the rate constants shown in Table 1, in reasonable agreement with earlier data of Chen and Stynes[9] for the dissociative solvolysis of **1** in toluene solution.

If this type of reaction is carried out in excess of the entering ligand (MeOH in our case) the observed first order rate constant is equal to the "off-rate" of the leaving ligand (MeIm). Solvolysis of the second MeIm does not take place since the *trans* effect of this ligand is much greater than that of MeOH.[9] Consequently, the first reaction observed spectrophotometrically is the solvolysis of ferroxime **1**, described by eqn. (2).

$$\text{[Fe(Hdmg)}_2\text{(MeIm)}_2\text{]} + \text{MeOH} \rightleftharpoons$$
$$\text{[Fe(Hdmg)}_2\text{(MeIm)(MeOH)]} + \text{MeIm} \quad (2)$$

In the presence of added H$_2$dbcat the spectral changes are the same as without H$_2$dbcat, *i.e.* only the solvolysis reaction (2) is observed.

Behaviour under O$_2$. Upon dissolution of [Fe(Hdmg)$_2$(MeIm)$_2$] **1** in methanol under O$_2$ the spectral changes shown in Fig. 1(a) are again observed, *i.e.* co-ordinated MeIm is lost in the same way as under N$_2$. The process obeys first-order kinetics with $k_{530} = 1.50 \times 10^{-2}$ s^{-1}, in agreement with the results under N$_2$. After that a slow spectral change occurs over 35 h, due to the formation of the μ-oxodiiron(III) derivative. The overall stoichiometry of the reaction of complex **1** with O$_2$ corresponds to eqn. (3) as demonstrated by volumetric

$$2\text{[Fe(Hdmg)}_2\text{(MeIm)}_2\text{]} + \tfrac{1}{2}\text{O}_2 \longrightarrow$$
$$\text{[O\{Fe(Hdmg)}_2\text{(MeIm)\}}_2\text{]} + 2\,\text{MeIm} \quad (3)$$
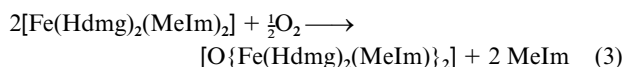
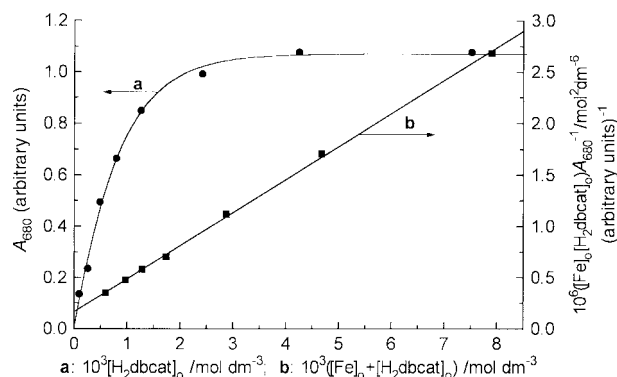determination of the dioxygen uptake. This reaction has not been investigated in detail.

Fig. 2 Variation of A_{680} as a function of [H$_2$dbcat]$_0$ (a), and the plot of eqn. (22) (b).

The μ-oxodiiron(III) dimer is only moderately reactive toward H$_2$dbcat. It is definitely not the active intermediate in the catalytic reaction. Upon addition of H$_2$dbcat to a solution aged under O$_2$ a slow production of dtbq is observed at 400 nm.

In the presence of an excess of MeIm (10% v/v) the solvolysis is markedly suppressed also under O$_2$. The successive spectra exhibit three isosbestic points (290, 470 and 580 nm). The 530 nm band decreases much more slowly, and to a lesser extent than in pure MeOH, producing a new shoulder at 360 nm, and new bands at 560 and 790 nm. The first order rate constants obtained at these wavelengths are in good agreement with each other (1.38×10^{-4}, 1.39×10^{-4} and 1.10×10^{-4} s^{-1} at 360, 530 and 790 nm, respectively), pointing to a single reaction. The appreciable decrease (approximately 100-fold) in the first order rate constant due to an increase in the excess of leaving ligand is consistent with the general kinetic equation for a dissociative mechanism (D) as discussed in ref. 9.

In the presence of H$_2$dbcat the successive spectra under O$_2$ first show the disappearance of the 530 nm band, but now the formation of a blue complex with a wide band centred at 680 nm can be observed. The 420 nm band is not visible, thus the solution does not contain appreciable amounts of complex **2**. The two isosbestic points (470 and 560 nm) indicate a single reaction, involving ferroxime, catechol and O$_2$.

The blue complex exhibits an ESR spectrum (room temperature, MeOH solution) consisting of a doublet ($g = 2.00425$ G, $a_{1H} = 3.135$ G), corresponding to the 3,5-di-*tert*-butylsemiquinone anion radical (dbsq$^{\cdot-}$) co-ordinated to the iron(II) nucleus of ferroxime. This is distinctly different from the ESR spectrum of free dbsq$^{\cdot-}$.[7a,b,e] In the absence of H$_2$dbcat, but under O$_2$ the only ESR signal detectable in MeOH solution was a singlet with $g = 2.1059$, which can be attributed to an iron-bound superoxo ligand.

In addition to its ESR spectrum, the nature of the blue complex can be rationalised on grounds of the facts that besides ferroxime(II) it requires the presence of *both* H$_2$dbcat and O$_2$, *i.e.* the catechol needs to be oxidised before being co-ordinated to the iron centre. The oxidation of ferroxime(II) to ferroxime(III) is not expected within the time of complex formation (*ca.* 1 min). These observations imply that the blue complex is formed from the 3,5-di-*tert*-butylsemiquinone anion radical generated immediately upon mixing the reactants.

In order to obtain information on the composition and stability constant of the blue complex, we carried out spectrophotometric titrations of [Fe(Hdmg)$_2$(MeIm)$_2$] with H$_2$dbcat under air at 640, 680 and 720 nm. The fast initial development of colour (absorbance jumps in 1 min) observed during titration gave saturation curves of the type shown in Fig. 2(a) for 680 nm. Linear plots of [Fe]$_0$[H$_2$dbcat]$_0$/A against ([Fe]$_0$ + [H$_2$dbcat]$_0$) were obtained at all of the three wavelengths, as illustrated by Fig. 2(b) for 680 nm. They were evaluated in terms of equilibrium (4) in combination with equations derived from the proposed mechanism (see below).
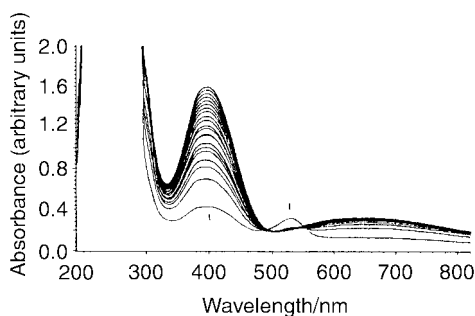
Fig. 3 Ferroxime-catalysed oxidation of H_2dbcat by O_2 monitored every 2 min ($l = 1$ mm). Formation of dtbq detectable at 400 nm. $[Fe(Hdmg)_2(MeIm)_2]_0 = 0.444 \times 10^{-3}$, $[H_2dbcat]_0 = 9.08 \times 10^{-3}$, $[O_2] = 1.1 \times 10^{-3}$ mol dm^{-3}.

Fig. 5 Initial rate of O_2 uptake (V_{in}) as a function of H_2dbcat concentration. $[Fe(Hdmg)_2(MeIm)_2]_0 = 0.24 \times 10^{-3}$, $[O_2] = 1.1 \times 10^{-3}$ mol dm^{-3}.
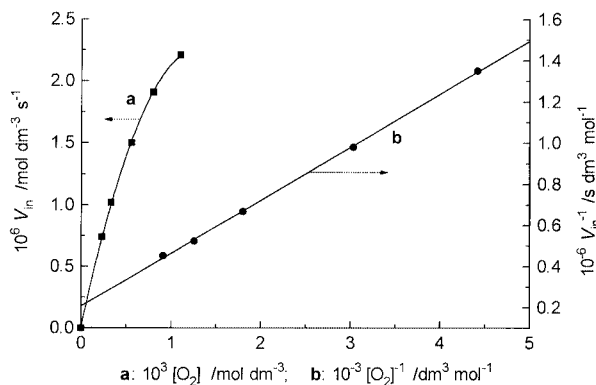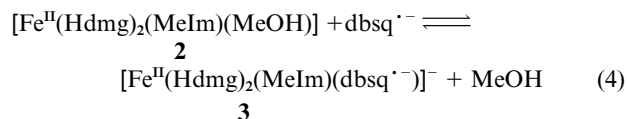

Fig. 4 Initial rate of O_2 uptake (V_{in}) as a function of dioxygen concentration (a), and plot of $1/V_{in}$ against $1/[O_2]$ (b). $[Fe(Hdmg)_2(MeIm)_2]_0 = 0.63 \times 10^{-3}$, $[H_2dbcat]_0 = 10.5 \times 10^{-3}$ mol dm^{-3}.

$$[Fe^{II}(Hdmg)_2(MeIm)(MeOH)] + dbsq^{\cdot-} \rightleftharpoons$$
$$\mathbf{2}$$
$$[Fe^{II}(Hdmg)_2(MeIm)(dbsq^{\cdot-})]^- + MeOH \quad (4)$$
$$\mathbf{3}$$

The blue complex **3** is the major ferroxime species during the steady state of the overall catalytic reaction. However, as will be demonstrated by the kinetic measurements, it is merely a *buffer* for ferroxime and dbsq$^{\cdot-}$, not being directly involved in reaction with O_2 to produce dtbq. In the steady state dtbq formation can be monitored by the growth of the 400 nm band (Fig. 3).

Kinetic measurements

Dioxygen absorption curves were recorded as a function of time in methanol as solvent for the dark blue solutions obtained in the presence of all components. From these curves the initial rates (V_{in}) of dioxygen uptake have been determined as a function of catalyst and substrate concentration as well as dioxygen partial pressure. The initial rate was found to be proportional to the catalyst concentration. When varying the concentration of dioxygen, we observed deviations from proportionality toward lower order, leading to a saturation type curve, which gave a linear double reciprocal plot of $1/V_{in}$ vs. $1/[O_2]$ (Fig. 4). Each point in the curve is the average of 3 individual runs reproducible to within ±5%. The dependence of V_{in} on $[H_2dbcat]_0$ is similar, but the rate reaches a limiting value (V_{lim}) at low ferroxime concentrations (Fig. 5), which can also be used for testing consistency with the proposed mechanism (see below).

The observed kinetic behaviour is consistent with the reaction mechanism in eqns. (2), (4)–(9), where for brevity Fe^{II}, Fe^{III} and Fe^{IV} denote the square-planar ferroxime moieties, Fe^{II}-(Hdmg)$_2$, [Fe^{III}(Hdmg)$_2$]$^+$ and [Fe^{IV}(Hdmg)$_2$]$^{2+}$, respectively, and N = MeIm. Co-ordinated MeOH is omitted except in step (2). According to this mechanism one of the MeIm ligands of
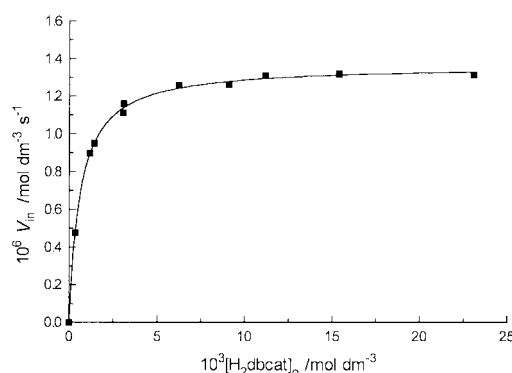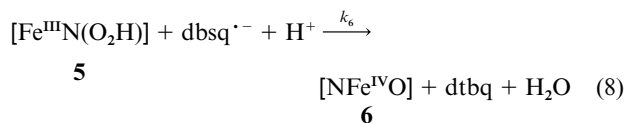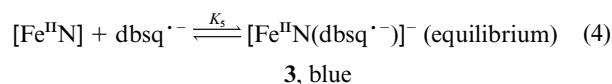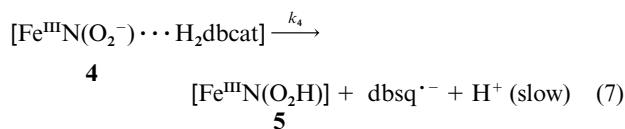
$$[Fe^{II}N_2] + MeOH \xrightarrow{K_1}$$
$$\mathbf{1}, violet$$
$$[Fe^{II}N(MeOH)] + N \text{ (solvolysis)} \quad (2)$$
$$\mathbf{2}, yellow$$

$$[Fe^{II}N] + O_2 \xrightleftharpoons{K_2} [Fe^{III}N(O_2^-)] \text{ (pre-equilibrium)} \quad (5)$$

$$[Fe^{III}N(O_2^-)] + H_2dbcat \xrightleftharpoons{K_3}$$
$$[Fe^{III}N(O_2^-) \cdots H_2dbcat] \text{ (pre-equilibrium)} \quad (6)$$
$$\mathbf{4}$$

$$[Fe^{III}N(O_2^-) \cdots H_2dbcat] \xrightarrow{k_4}$$
$$\mathbf{4}$$
$$[Fe^{III}N(O_2H)] + dbsq^{\cdot-} + H^+ \text{ (slow)} \quad (7)$$
$$\mathbf{5}$$

$$[Fe^{II}N] + dbsq^{\cdot-} \xrightleftharpoons{K_5} [Fe^{II}N(dbsq^{\cdot-})]^- \text{ (equilibrium)} \quad (4)$$
$$\mathbf{3}, blue$$

$$[Fe^{III}N(O_2H)] + dbsq^{\cdot-} + H^+ \xrightarrow{k_6}$$
$$\mathbf{5}$$
$$[NFe^{IV}O] + dtbq + H_2O \quad (8)$$
$$\mathbf{6}$$

$$[NFe^{IV}O] + H_2dbcat \xrightarrow{k_7} [Fe^{II}N] + dtbq + H_2O \text{ (fast)} \quad (9)$$
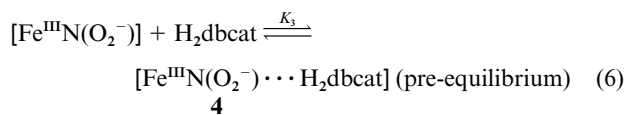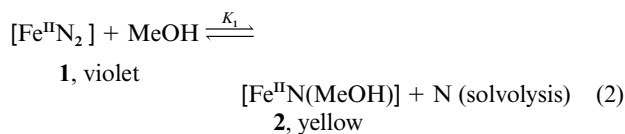
catalyst precursor **1** is lost *via* solvolysis, producing catalyst **2**, which then reversibly binds a dioxygen molecule, affording a superoxoiron(III) complex. The latter is capable of hydrogen bonding H_2dbcat to its external oxygen atom to form intermediate **4**, which undergoes intramolecular H-atom transfer in the rate-determining step, generating the semiquinone anion radical, dbsq$^{\cdot-}$, and a (hydrogenperoxo)iron(III) species. The dbsq$^{\cdot-}$ formed is either reversibly co-ordinated to the solvolysed ferroxime(II) **2**, forming the blue complex **3**, or is further oxidised in step (8) to the product dtbq.

In step (8) an electron from dbsq$^{\cdot-}$ is utilised for the proton-assisted reductive heterolytic splitting of the O–O bond of **5**, producing a reactive ferryl species **6**. The latter rapidly oxidises a second H_2dbcat molecule in step (9).

In the catalytic process steps (5) and (6) can be regarded as pre-equilibria and (7) as the rate-determining step. Reversibility is often encountered in dioxygen co-ordination to iron(II), which is in support of step (5). Hydrogen bonding to the super-oxo ligand is similar to that observed in the case of the analogous superoxocobaloxime(III).[7] The ferryl species formed is reactive enough to oxidise a catechol molecule.

To derive the kinetic equation corresponding to the proposed mechanism we need the mass balance for the ferroxime species and for H_2dbcat, which can be expressed by eqns.(10) and (11),

$$[Fe]_0 = [Fe^{II}N_2] + [Fe^{II}N] + [Fe^{II}N(O_2^-)] + [4] +$$
$$[Fe^{II}N(O_2H)] + [Fe^{II}N(dbsq^{\cdot-})] + [NFe^{IV}O] \quad (10)$$

$$[H_2dbcat]_0 = [H_2dbcat] + [Fe^{II}N(dbsq^{\cdot-})] +$$
$$[dbsq^{\cdot-}] + [dtbq] \quad (11)$$

respectively. In the steady state, the solvolysis of $[Fe^{II}N_2]$ is complete, therefore, the first term in eqn. (10) can be neglected. The concentrations of species $[Fe^{II}N(O_2H)]$ and $[NFe^{IV}O]$ are assumed to be negligible owing to their high reactivity. In view of the results of spectrophotometric titrations, $[Fe^{II}N(dbsq^{\cdot-})]$ is the predominant ferroxime species in the reacting solutions, amounting to an average of 90% of the overall ferroxime concentration at the excesses of H_2dbcat used in the measurements ($a \approx 0.9$). The simplified mass balance will thus have the form of eqn. (12).

$$[Fe]_0 - [Fe^{II}N(dbsq^{\cdot-})] = (1 - a)[Fe]_0 =$$
$$[Fe^{II}N] + [Fe^{II}N(O_2^-)] + [4] \quad (12)$$

Combination of the mass balance for the ferroxime species with the expressions for equilibria (5) and (6), the mechanism (2), (4)–(9) leads to kinetic equation (13). Owing to the excess of

$$V_{in} = k_4[4] = \frac{k_4 K_2 K_3 [O_2][H_2dbcat](1 - a)[Fe]_0}{1 + K_2[O_2](1 + K_3[H_2dbcat])} \quad (13)$$

H_2dbcat over ferroxime, $[H_2dbcat] \approx [H_2dbcat]_0$ and $1 \ll K_3[H_2dbcat]$ within the parentheses. This leads to the simplified kinetic equation (14). The linear plot of $1/V_{in}$ vs. $1/[O_2]$ (Fig. 4)

$$V_{in} = \frac{k_4 K_2 K_3 [O_2][H_2dbcat]_0(1 - a)[Fe]_0}{1 + K_2 K_3 [O_2][H_2dbcat]_0} \quad (14)$$

allows one to determine k_4 from the intercept and subsequently $K_2 K_3$ from the slope. The results are collected in Table 2.

Using eqn. (14), the limiting initial rate reached at sufficiently high H_2dbcat concentration can be expressed as in eqn. (15),

$$V_{in,lim} = k_4(1 - a)[Fe]_0 \quad (15)$$

which is an additional source of k_4 (Table 2) where $a = [3]/[Fe]_0$, having an average value of 0.9 in the interval of the limiting rate. The slope of the V_{in} vs. $[Fe]_0$ plot can be calculated from the known constants in eqn. (14) and compared with its experimental value. The good agreement (Table 2) provides additional support for the proposed reaction mechanism (2), (4)–(9).

The mechanism suggested is also consistent with results of the spectrophotometric titrations shown in Fig. 2. The linear plot obtained can be interpreted by assuming that the only species absorbing at these wavelengths are ferroxime 2, and the semiquinonato complex 3 formed in equilibrium (4) [eqn. (16)].

$$A = l\varepsilon_3[Fe^{II}N(dbsq^{\cdot-})] + l\varepsilon_2[Fe^{II}N] \quad (16)$$

$$[Fe]_0 = [Fe^{II}N] + [Fe^{II}N(dbsq^{\cdot-})] \quad (17)$$

$$[H_2dbcat]_0 = [H_2dbcat] + [dbsq^{\cdot-}] + [Fe^{II}N(dbsq^{\cdot-})] \quad (18)$$

$$[dbsq^{\cdot-}] = k_4[4]/k_5[Fe^{II}N] \quad (19)$$

$$K_5 = [Fe^{II}N(dbsq^{\cdot-})]/[Fe^{II}N][dbsq^{\cdot-}] \quad (20)$$

Table 2 Rate and equilibrium constants for mechanism (5)–(9) ($T = 25\ °C$)

Constant	Value	Source
k_4	$(7.70 \pm 0.30) \times 10^{-3}\ s^{-1}$	Intercept, Fig. 4
	$(6.88 \pm 0.28) \times 10^{-3}\ s^{-1}$	Limiting rate, Fig. 5
$K_2 K_3$	$(7.58 \pm 0.35) \times 10^4\ dm^6\ mol^{-2}$	Slope, Fig. 4
Slope, V_{in} vs. $[Fe]_0$	$(3.54 \pm 0.2) \times 10^{-3}\ s^{-1}$	Measured
	$(3.68 \pm 0.2) \times 10^{-3}\ s^{-1}$	Calculated [a]
k_{-5}	$(8.14 \pm 0.32) \times 10^{-5}\ s^{-1}$	Calculated [b]
K^*	$(1.41 \pm 0.02) \times 10^3\ dm^3\ mol^{-1}$	Slope, Fig. 2(b)

[a] Using k_4 and $K_2 K_3$ obtained from Fig. 4. [b] From eqn. (21), using $K_5 = k_5/k_5$.

Table 3 Stability constant and molar absorbance of $[Fe^{II}N(dbsq^{\cdot-})]$ at three wavelengths

λ/nm	$\Delta\varepsilon/dm^3\ mol^{-1}\ cm^{-1}$	$10^{-3}\ K^*/dm^3\ mol^{-1}$
640	3150 ± 120	1.44 ± 0.08
680	3270 ± 95	1.38 ± 0.06
720	3030 ± 110	1.42 ± 0.06

$$K^* = K_2 K_3 K_5 [O_2] k_4 / k_5 = [Fe^{II}N(dbsq^{\cdot-})] /$$
$$[Fe^{II}N][H_2dbcat] \quad (21)$$

$$[Fe]_0 [H_2dbcat]_0 / A = (K^*/\Delta\varepsilon)([Fe]_0 + [H_2dbcat]_0) +$$
$$(1/\Delta\varepsilon) \quad (22)$$

(For $dbsq^{\cdot-}$ at 680 nm, $\varepsilon_{sq} = 140\ dm^3\ mol^{-1}\ cm^{-1}$.) At the early stages of the reaction (after mixing of the reactants with H_2dbcat in *ca.* 1 min), where the measurements were made, simplified balance conditions (17) and (18) are valid. Based on the proposed mechanism, assuming that $k_4[4] \gg k_{-5}[3]$ and $k_5[2] \gg k_6[5]$, the concentration of $dbsq^{\cdot-}$ can be expressed from the steady-state conditions by eqn. (19). Combining eqns. (16)–(19), the concentrations on the right-hand side of eqn. (20) can be expressed by measurable quantities. Neglecting the product $[3] \times [3]$ in the resulting expression, eqn. (22) is obtained, where $\Delta\varepsilon = \varepsilon_3 - \varepsilon_2$.
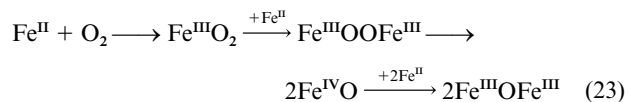
If this model is correct, the plot of the left-hand side of eqn. (22) against $([Fe]_0 + [H_2dbcat]_0)$ should be linear, which is indeed the case (Fig. 2b). From the slopes and intercepts at three wavelengths, we have obtained the stability constants K^* and $\Delta\varepsilon \approx \varepsilon_3 - \varepsilon_{sq}$ listed in Table 3. From the results $K^* = (1.41 \pm 0.02) \times 10^3\ dm^3\ mol^{-1}$.

The co-ordination sphere of the square planar ferroxime(II) is structurally similar to that of various iron porphyrin species found in heme type monooxygenases, which also possess catecholase activity. The mechanism (2), (4)–(9) found consistent with the observed kinetic behaviour of ferroxime(II) is in several aspects similar to the known mechanism of dioxygen activation by cytochrome P-450.[1] There are three active intermediates in the catalytic oxidation: (i) the superoxoferroxime(III), (ii) the (hydrogenperoxo)ferroxime(III) 5, formed *via* H-atom abstraction by the superoxo species, and (iii) the ferryl species $[NFe^{IV}=O]$, which is formed *via* heterolytic cleavage of 5. The analogues of these intermediates are known from the generally accepted mechanism for cytochrome P-450, where (i) and (ii) correspond to species produced by the external electron source required for enzyme action. In the present case H_2dbcat serves as both reducing agent and substrate.

The generation of $dbsq^{\cdot-}$ by superoxoferroxime(III) is a feature analogous to the cobaloxime(II)–H_2dbcat–O_2 system studied by us in detail.[7] This propensity of superoxo complexes is similar to the well known reaction of organic peroxyl radicals

ROO· with H-atom donors. Stabilisation of the anion radical by delocalisation contributes strongly to the driving force of H-atom transfer.

In absence of a single-electron (H-atom) source, the superoxoferroxime(III) behaves as predicted by the known general scheme (23) for iron-based oxidant systems.[1] It reacts with **1**,

$$Fe^{II} + O_2 \longrightarrow Fe^{III}O_2 \xrightarrow{+Fe^{II}} Fe^{III}OOFe^{III} \longrightarrow$$

$$2Fe^{IV}O \xrightarrow{+2Fe^{II}} 2Fe^{III}OFe^{III} \quad (23)$$

affording a μ-peroxodiiron(III) species, which undergoes homolytic splitting to the ferryl derivative followed by combination with **1**, leading to the μ-oxodiiron(III) end product, eqn. (23) (ligands omitted for clarity).

The oxidation potentials and kinetic labilities of these intermediates govern the ability of an iron complex to catalyse substrate oxidation by O_2. Depending on their chemical nature and structural features, various substrates may be capable of reducing one or more intermediate(s), thereby determining the activity and selectivity observed in a given system.

Work is in progress further to explore the reactivities of ferroxime type complexes in catalytic oxidations.

Acknowledgements

References

1 L. Que, Jr., *Coord. Chem. Rev.*, 1983, **50**, 73; in *Bioinorganic Catalysis*, ed. J. Reedijk, Marcel Dekker, New York, 1993, pp. 347–393; C. G. Pierpont and C. W. Lange, *Prog. Inorg. Chem.*, 1994, **41**, 331; L. I. Simándi, *Catalytic Activation of Dioxygen by Metal Complexes*, Kluwer Academic Publishers, Dordrecht, Boston, London, 1992, ch. 6; T. Funabiki, in *Oxygenases and Model Systems*, ed. T. Funabiki, Kluwer Academic Publishers, Dordrecht, Boston, London, 1997, pp. 19–104, 105–156.
2 D. Mansuy and P. Battioni, in *Bioinorganic Catalysis*, ed. J. Reedijk, Marcel Dekker, New York, 1993, p. 395.
3 *Metalloporphyrins in Catalytic Oxidation*, ed. R.A. Sheldon, Marcel Dekker, New York, 1994.
4 H. Noglik, D. W. Thompson and D. V. Stynes, *Inorg. Chem.*, 1991, **30**, 4571.
5 I. Vernik and D. V. Stynes, *Inorg. Chem.*, 1996, **35**, 1093.
6 H. E. Toma and A. C. C. Silva, *Can. J. Chem.*, 1986, **64**, 1280.
7 (*a*) L. I. Simándi, T. Barna, L. Korecz and A. Rockenbauer, *Tetrahedron Lett.*, 1993, **34**, 717; (*b*) L. I. Simándi, T. Barna, Gy. Argay and T. L. Simándi, *Inorg. Chem.*, 1995, **34**, 6337; (*c*) L. I. Simándi, T. Barna and S. Németh, *J. Chem. Soc., Dalton Trans.*, 1996, 473; (*d*) L. I. Simándi and T. L. Simándi, *J. Mol. Catal. A: Chemical*, 1997, **117**, 299; (*e*) L. I. Simándi and T. L. Simándi, *J. Chem. Soc., Dalton Trans.*, 1998, 3275.
8 I. W. Pang and D. V. Stynes, *Inorg. Chem.*, 1977, **16**, 590.
9 X. Chen and D. V. Stynes, *Inorg. Chem.*, 1986, **25**, 1173.